Role of the *Atg9a* gene in intrauterine growth and survival of fetal mice

Takashi Kojima[a], Takahiro Yamada[a], Rina Akaishi[a], Itsuko Furuta[a], Tatsuya Saitoh[b], Kazuhiko Nakabayashi[c], Kei-Ichi Nakayama[d], Keiko Nakayama[e], Shizuo Akira[b], Hisanori Minakami

[a]Department of Obstetrics, Hokkaido University Graduate School of Medicine, Sapporo, 060-8638, Japan; [b]Laboratory of Host Defense, WPI Immunology Frontier Research Centre, Osaka University, Suita, 565-0871, Japan; [c]Division of Developmental Genomics, Department of Maternal-Fetal Biology, National Centre for Child Health and Development, Tokyo, Japan; [d]Department of Molecular and Cellular Biology and Laboratory of Embryonic and Genetic Engineering, Medical Institute of Bioregulation, Kyushu University, Fukuoka, 812-8582, Japan; [e]Division of Cell Proliferation, Tohoku University School of Medicine, Sendai, 980-8575, Japan

Short title: *Atg9a* gene in murine fetal growth and survival

Corresponding author:

Takahiro Yamada

E-mail address: taka0197@med.hokudai.ac.jp

Phone number: +81-11-706-5941

Current address: N15W7, Kita-ku, Sapporo, 060-8638, Japan

Abstract

Autophagy is activated by environment unfavorable for survival and requires Atg9a protein. Mice heterozygous for $p57^{Kip2}$, devoid of the imprinted paternal allele ($p57^{Kip2+/-}$), are known to develop hypertension during pregnancy. To determine whether fetal *Atg9a* is involved in the intrauterine survival and growth of fetal mice, this study was performed on *Atg9a* heterozygous ($Atg9a^{+/-}$) pregnant mice with and without $p57^{Kip2+/-}$. The pregnant mice heterozygous for both knockout alleles of *Atg9a* and $p57^{Kip2}$ ($Atg9a^{+/-}$/$p57^{Kip2+/-}$), but not those heterozygous for *Atg9a* alone, developed hypertension during pregnancy. Placental expression of *Atg9a* mRNA was significantly decreased in the $Atg9a^{-/-}$ mice compared to $Atg9a^{+/-}$ or $Atg9a^{+/+}$ mice. The $Atg9a^{-/-}$ fetal mice exhibited significantly retarded growth and were more likely to die *in utero* compared to $Atg9a^{+/+}$ and $Atg9a^{+/-}$ fetal mice. Growth retardation was observed in the presence of maternal hypertension in $Atg9a^{-/-}$ fetal mice. These results suggest that $Atg9a^{-/-}$ fetal mice from pregnant dams heterozygous for both knockout alleles of *Atg9a* and $p57^{Kip2}$ are more susceptible to hypertensive stress than fetuses with intact autophagic machinery.

Key words: Autophagy, Fetal growth restriction, Hypoxia, Intrauterine fetal death, Hypertension

1. Introduction

Autophagy is a bulk degradation system, which controls the clearance and reuse of intracellular constituents, and is important for the maintenance of an amino acid pool essential for survival [1-3]. Autophagy can be activated by nutritional deprivation and intracellular stress, such as hypoxia. Genetic studies in yeast have identified many autophagy-related (*Atg*) genes that are required for autophagosome formation essential for autophagy, such as *Atg3*, *Atg5*, *Atg7*, *Atg9a*, and *Atg16L1* [4]. Most of the *Atg* genes are conserved in higher eukaryotes. In yeast, autophagy-defective mutants were unable to survive under conditions of nitrogen starvation [5]. Similarly, the *Atg3*-, *Atg5*-, *Atg7*-, *Atg9a*-, and *Atg16L1*-knockout mice (genotypes of each *Atg* $^{-/-}$) did not survive, and usually died within **one** day after birth [6-9]. Thus, autophagy was found to be crucial for survival in the neonatal period [6-10], while mice heterozygous for the knockout allele of the *Atg9a* gene (*Atg9a*$^{+/-}$) grew normally [9]. Even in the embryonic stages, a shortage of nutrient and oxygen supply from the placenta occurs in human fetuses in certain clinical conditions, such as hypertensive pregnancies and maternal malnutrition, leading to fetal growth restriction (FGR) and intrauterine fetal death (IUFD) [11-13]. Therefore, similar adverse events may occur in response to unfavorable intrauterine environments in fetal mice devoid of autophagic machinery. Indeed, FGR and IUFD have been reported in fetal mice deficient in *beclin 1*, which is another gene essential for autophagy [14].

The *Atg9b* gene - expressed in the placenta - functionally complements *Atg9a* [19]. Therefore, Atg9b protein expression may be higher in the placenta of *Atg9a*$^{-/-}$ fetal mice.

When the expression of Atg9b protein is increased, autophagic activity may be monitored by quantifying the expression of LC3-II (truncated protein of LC3-I) in the placenta of *Atg9a*$^{-/-}$ fetal mice.

The p57^{Kip2}, a potent inhibitor of the cyclin-cyclin dependent kinase (CDK) complex, is a paternally imprinted gene located within a cluster of imprinted genes in humans (chromosome 11p15.5) and mice (distal chromosome 7) [15,16]. As p57$^{Kip2+/-}$ (heterozygous, lacking the paternal allele) pregnant mice develop abnormalities similar to preeclampsia, including hypertension and proteinuria when carrying a fetus without p57^{Kip2} expression [17], these mice can be used as an animal model for hypertensive disorders in pregnancy. The present study was performed to determine whether fetal *Atg9a* is involved in survival and *in utero* growth in pregnant mice heterozygous for *Atg9a* (*Atg9a* $^{+/-}$) with and without p57$^{Kip2+/-}$. In addition, expressions of *Atg9b* mRNA, Atg9b protein and LC3-II protein were compared between placentas with *Atg9a*$^{-/-}$ and *Atg9a*$^{+/+}$.

2. Materials and Methods

2.1. Mice

Mice housed in a temperature- and humidity-controlled room were maintained under a 12:12-hour light-dark schedule with free access to food and water. All procedures were performed in accordance with the Local Ethical Commission for Animal Experiments at Hokkaido University (Japan). Female and male mice (129Sv × C57BL/6) heterozygous for *Atg9a* (*Atg9a*$^{+/-}$) [9] were provided by a co-author (TS). Male mice heterozygous for p57^{Kip2},

lacking the imprinted paternal allele ($p57^{Kip2+/-}$) [18], were provided by co-authors (KN and KN). In the current study, female mice of *Atg9a* $^{+/-}$ alone were mated with male mice of $p57^{Kip2\,+/-}$ to generate female mice heterozygous for knockout alleles of *Atg9a* and $p57^{Kip2}$ (*Atg9a* $^{+/-}$/$p57^{Kip2\,+/-}$). The genotype of generated *Atg9a* $^{+/-}$/$p57^{Kip2\,+/-}$ female was determined by PCR of tail DNA. Female mice of *Atg9a* $^{+/-}$ and *Atg9a* $^{+/-}$/$p57^{Kip2\,+/-}$ were mated with male mice of *Atg9a* $^{+/-}$ to generate four embryo groups (groups A1, A2, B1 and B2, Tab. 1) divided according to differences in mother and fetal *Atg9a* genotypes. Pregnancy stage was expressed as the number of days *post coitum* (dpc). Thirteen pregnant mice with *Atg9a* $^{+/-}$ and 13 pregnant mice with *Atg9a* $^{+/-}$/$p57^{Kip2\,+/-}$ were used in the study. Pregnant mice of both groups were sacrificed on 13.5, 15.5, and 17.5 dpc for determination of the number of fetuses, measurement of live fetal body weight and determination of fetal *Atg9a* genotypes by PCR of tail DNA (Fig. 1).

2.2. Measurement of blood pressure in pregnant mice

Blood pressure was measured with a tail-cuff using a CODA™ monitor (Kent Scientific, Torrington, CT, USA), 5 – 10 times at 30 s intervals, 15 min after the behavior and heart rate of the pregnant mice were stabilized in the morning of 5.5, 9.5, 13.5, 15.5, and 17.5 dpc. Blood pressure values are reported as the means of at least three measurements varying by 5% obtained in one session.

83 **2.3. Measurement of fetal body weight**

84 The body weights of pregnant mice and alive fetal mice were measured using Electronic
85 balance FA-200 (A&D, Tokyo, Japan). Pregnant mice were anesthetized deeply with ether
86 and dissected in the lower abdomen. The multilocular uterus containing a fetus in each
87 loculus was incised and fetuses with their placentas were separated from the uterus. Some
88 fetuses, based on their color and size, appeared to be dead at sacrifice. Fetuses that were less
89 pinkish and smaller than others were judged as dead (Fig. 1; upper panel). These fetuses were
90 subjected to *Atg9a* genotype determination, but their body weights were not measured.

91

92 **2.4. DNA extraction, PCR amplification and electrophoresis**

93 The *Atg9a* genotypes of the fetuses (Fig. 1; lower panel) and placentas were analyzed using
94 PCR of fetal tail DNA and placental DNA. The DNA was extracted using a DNA extraction
95 kit (DNeasy® Blood & Tissue Kit; Quiagen, Valencia, CA, USA). PCR was performed in a
96 final volume of 15 μL consisting of 1 μL of genomic DNA, 1.5 μL of 10× Taq buffer, 1.5 μL
97 of dNTPs (2.5 mM each), 0.6 μL each of forward and reverse primers, 9.7 μL of nuclease-free
98 water, and 0.1 μL of Taq DNA polymerase, under the following conditions: 3 min at 95°C, 35
99 cycles at 95°C for 20 s and 68°C for 1 min. The primers for the wild-type allele were**:**
100 5'-CCAGAGCCTGTCATGGTACTGGGAACC-3' (primer I) and
101 5'-CCTCAAGGAGCAGGTGCAGCGAGATGG-3' (primer II). For the knockout allele,
102 primer I and 5'-CTAAAGCGCATGCTCCAGACTGCCTTG-3' (primer III) were used. The
103 amplified products were checked by 2.0% agarose gel electrophoresis with ethidium bromide.

The DNA bands were visualized with a UV transilluminator to determine the genotypes (Fig. 1; lower panel).

2.5. Detection of *Atg9b* mRNA expression

The RNA samples were extracted from 20 mg of frozen placental sample using an RNeasy® Plus Mini Kit (Qiagen) after smashing with MicroSmash™ (Tomy Seiko, Tokyo, Japan), and the sample RNA concentrations were measured by NanoDrop® (ND-1000; Thermo Scientific Japan, Kanagawa, Japan). After dilution of each sample with RNase-free water and adjusted to a uniform density (3 μg/μL), reverse-transcription polymerase chain reaction (RT-PCR) was performed with Super Script™ III (Life Technologies, Carlsbad, CA, USA). Quantitative Real-time PCR was used to measure the expression of *Atg9b* mRNA using SYBR® Premix Ex Taq™ (Takara, Shiga, Japan) and an ABI 7300 Real-Time PCR System (PE Applied Biosystems, Foster City, CA, USA). *GAPDH* was used as an internal standard (housekeeping gene). Real-time PCR was performed in a final volume of 15 μL consisting of 0.6 μL of sample cDNA, 7.5 μL of 2x Ex Taq buffer, 0.3 μL of 50x ROX Reference Dye, 0.6 μL each of forward and reverse primers, 5.4 μL of nuclease-free water under the following conditions: for *Atg9a*, 2 min at 50°C, 10 s at 95°C, 40 cycles at 95°C for 15 s and 59°C for 1 min; and for *Atg9b* and *GAPDH*, 2 min at 50°C, 10 s at 95°C, 40 cycles at 95°C for 15 s and 62°C for 1 min. The sequences of primers were 5'-GAGCAGGTGCAGCGAGATG-3'(forward) and 5'-GCAGGTCTCTGGACAGTGAGG-3' (reverse) for *Atg9a*,

124 5’-GCATCACATCCAGAACCTGGA-3’ (forward) and

125 5’-CCGCTGATGATAGCTGTAGATCTTG-3’ (reverse) for *Atg9b*, and

126 5’-GGCATTGCTCTCAATGACAA-3’ (forward) and 5’-TGTGAGGGAGATGCTCAGTG-3’

127 (reverse) for *GAPDH*.

128

129 **2.6. Immunodetection of Atg9b and LC3-II**

130 Western blotting was performed to analyze the expression levels of Atg9b protein and

131 microtubule-associated protein light chain 3 (LC3)-II (truncated protein of LC3-I). The

132 sample proteins were extracted from 20 mg of frozen placental tissues after mixing with 100

133 μL of 2% Triton X-100 lysis buffer (20 mM Tris-HCl, 150 mM NaCl, 2% Triton X-100, 2

134 mM PMSF, and complete protease inhibitor cocktail), and then sonicated (Handy Sonic®;

135 Tomy Seiko, Tokyo, Japan), extracted, and the protein concentration was measured by BCA

136 Protein Assay (Thermo Fisher Scientific, Rockford, IL, USA).

137 Aliquots of 12 μg of protein samples were diluted with 1:2 volumes of Laemmli

138 sample buffer (10% SDS, 1 M DTT, 0.5 M Tris-HCl, pH 6.8, 0.001% bromophenol blue, and

139 5% glycerol), boiled at 95°C for 5 min, separated by SDS-polyacrylamide gel electrophoresis

140 (SDS-PAGE) using 8% gels for Atg9b and 13% for LC3-II, electrotransferred onto PDVF

141 membranes (Amersham Biosciences, Little Chalfont, UK), and blocked with 1.5% skim milk

142 in TBS-T (1× TBS with 0.08% Tween) at room temperature for 60 min. The membranes were

143 incubated with the following primary antibodies at 4°C overnight: Atg9b (anti-ATG9B

antibody, 1:1000; NB110-74833; NOVUS, Littleton, CO, USA), LC3-II (anti-LC3, 1:800; MBL, Nagoya, Japan). GAPDH was also detected as a loading control in this study using an anti-GAPDH mouse IgG antibody at a dilution of $1:4\times10^6$.

After washing with TBS-T, the membranes were incubated with secondary antibody at room temperature for 60 min. ECL™ anti-rabbit IgG, horseradish peroxidase-conjugated whole antibody (1:10000; GE Healthcare, Little Chalfont, UK) was used for Atg9b and LC3-II, and ECL™ anti-mouse IgG, horseradish peroxidase-conjugated whole antibody (1:10000; GE Healthcare) for GAPDH. The protein bands were visualized with ECL solution (Immobilon™ Western, Chemiluminescent HRP Substrate; Millipore, Little Chalfont, UK) and quantified with ImageQuant LAS4000 (GE Healthcare Japan, Tokyo, Japan).

2.7. Statistical analysis

Data are presented as mean±standard deviation. Statistical analysis was performed using the JMP© Pro 11 statistical software package (SAS, Cary, NC, USA). Differences between two groups were tested using the Mann-Whitney U test (Figs. 2, 5, and 6). Differences between more groups were tested using the Steel-Dwass test after confirmation of significant difference with Kruskal-Wallis test (Figs. 3, 4, and 7). Differences between frequencies were tested using Fisher's exact test with Bonferroni correction (Table 2). In all analyses, $P < 0.05$ was taken to indicate statistical significance.

3. Results

Atg9a$^{+/-}$ mice (used to obtain A1 and A2 groups, Tab. 1) did not exhibit significant changes in systolic blood pressure (SBP) during pregnancy (Fig. 2), while *Atg9a*$^{+/-}$/p57$^{Kip2\,+/-}$ mice (used to obtain B1 and B2 groups, Tab. 1) exhibited a significant increase in SBP at 9.5 dpc (113 ± 11.6 mm Hg) and thereafter (116 ± 12.6, 125 ± 16.2, and 121 ± 12.8 mm Hg for 13.5, 15.5, and 17.5 dpc, respectively) compared to SBP baseline (102 ± 12.0 mm Hg) determined before pregnancy. The SBP differed significantly between the two groups (A *vs*. B) at 9.5 dpc (113 ± 11.6 *vs*. 99 ± 9.5 mm Hg), 15.5 dpc (125 ± 16.2 *vs*. 95 ± 10.5 mm Hg), and 17.5 dpc (121 ± 12.8 *vs*. 102 ± 12.1 mm Hg). Pre-pregnancy body weight did not differ significantly between female mice of *Atg9a*$^{+/-}$ (normotensive pregnancy [A] group; n=13; Tab. 1) and *Atg9a*$^{+/-}$/p57$^{Kip2\,+/-}$ (hypertensive pregnancy group [B]; n=13) groups (22.8 ± 2.7 *vs*. 21.7 ± 2.5 g, respectively).

The expression of *Atg9a* mRNA was significantly reduced in *Atg9a*$^{-/-}$ placentas compared to *Atg9a*$^{+/-}$ and *Atg9a*$^{+/+}$ placentas (Fig. 3). Then, placental expression of *Atg9b* mRNA, Atg9b protein and LC-3-II protein (Fig. 4) were analyzed in relation to placental *Atg9a* genotype (*Atg9a*$^{+/+}$ *vs*. *Atg9a*$^{-/-}$) and the presence or absence of gene *p57*$^{Kip2\,+/-}$ (indicative of hypertension). The *Atg9b* mRNA expression in *Atg9a*$^{-/-}$ placentas was comparable to that of *Atg9a*$^{+/+}$ placentas. However, in the presence of hypertension, the *Atg9b* mRNA level was significantly higher in *Atg9a*$^{+/+}$ placentas than that in *Atg9a*$^{-/-}$ placentas. The expression of Atg9b and LC3-II proteins was significantly higher in *Atg9a*$^{-/-}$ placentas than in *Atg9a*$^{+/+}$ placentas in the presence of hypertension (Fig. 4).

The *Atg9a*$^{+/+}$, *Atg9a*$^{+/-}$, and *Atg9a*$^{-/-}$ fetal mice accounted for 30% (69/231), 53%

186 (123/231), and 17% (39/231) of the total number of fetuses, respectively, with the number of
187 *Atg9a*$^{-/-}$ fetal mice lower than the expected Mendelian frequency (Tab. 2). The fraction of
188 dead fetal mice appeared to be greater with decreasing number of fetal *Atg9a* alleles: 1.4%
189 (1/69), 14% (17/123), and 26% (10/39) for *Atg9a*$^{+/+}$, *Atg9a*$^{+/-}$, and *Atg9a*$^{-/-}$ fetuses,
190 respectively. The prevalence rate of IUFD was significantly higher in *Atg9a*$^{-/-}$ fetal mice than
191 in *Atg9a*$^{+/+}$ fetal mice (26% [10/39] *vs.* 1.4% [1/69]) and in fetal mice with at least one *Atg9a*
192 allele (*Atg9a*$^{+/+}$ + *Atg9a*$^{+/-}$) (26% [10/39] *vs*. 9.4% [18/192]).
193 The fetal body weight was significantly lower in fetuses carried by hypertensive
194 dams than those of normotensive dams (B1 and B2 < A1 and A2) at all stages of pregnancy
195 (Fig. 5). The fetal body weight was also significantly lower in *Atg9a*$^{-/-}$ fetal mice (groups A2+
196 B2) than in *Atg9a* $^{+/+}$ and *Atg9a* $^{+/-}$ fetal mice (groups A1 +B1) on 13.5 and 17.5 dpc (Fig. 6).
197 Finally, the body weight of fetuses carried by hypertensive dams was usually lower than that
198 fetuses of normotensive dams (Fig. 7). At any stage of pregnancy, fetal body weight did not
199 differ between the groups carried by normotensive dams (A1 *vs*. A2). In contrast, body weight
200 of fetuses carried by hypertensive dams was significantly lower in group B2 than in group B1
201 on 15.5 and 17.5 dpc (Fig. 7).
202
203 **4. Discussion**
204 The current study demonstrated that the growth of *Atg9a* $^{-/-}$ fetal mice was retarded compared
205 with *Atg9a* $^{+/+}$ and *Atg9a* $^{+/-}$ fetal mice. This confirmed the results of previous studies in which
206 autophagy-defective fetal mice devoid of *Atg* genes other than *Atg9a* were born with lower

207 birth weight than those with normal (in relation to autophagy) phenotype [6,7,10]. In addition,
208 it was suggested that *Atg9a*-knockout fetal mice are characterized by an increased likelihood
209 of dying *in utero*, as it was reported for *beclin 1*-knockout fetal mice [14].

210 Since in mice autophagy remains at a low level throughout the embryonic period
211 and massive autophagy occurs transiently soon after birth in normal neonatal mice, autophagy
212 was suggested to play minor role in fetal mouse development [6]. Therefore, fetal growth
213 restriction of *Atg9a*-knockout fetal mice has not been emphasized in previous reports [6,7,10].
214 The body weights of *Atg3* $^{-/-}$, *Atg5* $^{-/-}$, and *Atg7* $^{-/-}$ neonatal mice were significantly lower
215 than those of wild-type and heterozygous mice [6,7,10]. As all *Atg3* $^{-/-}$, *Atg5* $^{-/-}$, *Atg7* $^{-/-}$, and
216 *Atg9a* $^{-/-}$ mice are indeed defective in autophagy [6,7,9,10], these results suggest that the lack
217 of functional autophagic machinery in fetuses resulted in a lower birth weight. Thus, the fetal
218 autophagic machinery has a protective function against FGR. This notion was further
219 supported by our findings that FGR was observed in *Atg9a*$^{-/-}$ fetal mice carried by
220 hypertensive dams.

221 Although in the current study, the fetus size in normotensive dams did not differ
222 significantly among different fetal *Atg9a* genotype, the Atg9b and LC3-II proteins were
223 present in the placentas of *Atg9a*$^{-/-}$ fetal mice. The placental autophagy may have prevented
224 FGR in *Atg9a*$^{-/-}$ fetal mice carried by normotensive dams. The deleterious effect of
225 hypertension in addition to the lack of fetal autophagy, in turn, may have outweighed the
226 protective effect of placental autophagy on FGR in fetuses carried by hypertensive dams.

227 Maternal hypertension is a well-known detrimental factor for pregnancy outcome,

228 causing FGR and IUFD in humans [12]. Placental insufficiency due to poor blood supply *via*
229 the uterine arteries is the most common cause of fetal starvation, and the increased impedance
230 to flow within uterine arteries occurs frequently in hypertensive disorders in pregnancy
231 [11,13]. In such an unfavorable intrauterine environment, fetal autophagy may be activated,
232 and placental autophagy was indeed increased in women with hypertensive disorders and/or
233 FGR [20-24]. In addition, the expression of LC3-II protein in the human placenta tended to
234 linearly increase with a decreasing normalized infant birth weight [24]. The findings in
235 humans and mice suggest that dysfunction of the fetal autophagic machinery is causally
236 associated with FGR, and an unfavorable intrauterine environment such as maternal
237 hypertension outweighs the protective role of fetal autophagy in FGR, leading to FGR even
238 after the activation of autophagy.

239 The *Atg9a* $^{-/-}$ fetal mice had a high likelihood of *in utero* death in the present study.
240 In addition, the frequency of *Atg9a* $^{-/-}$ fetal mice was somewhat lower than the expected
241 Mendelian frequency, even after including dead fetuses. Similar findings, but with a more
242 severe phenotype, were reported in *beclin 1*-knockout fetal mice. No homozygous mutant
243 offspring (*beclin 1* $^{-/-}$) were born to dams heterozygous for *beclin 1* because all *beclin 1* $^{-/-}$
244 fetal mice had severely retarded growth and died in the early embryonic stages [14]. Such
245 early-dead fetuses become conceptus traces and are not recognized as fetuses [14]. These
246 early embryonic deaths may help to explain why less *Atg9a* $^{-/-}$ fetal mice than expected were
247 observed in the current study. In addition, strict classification of fetal mice as dead or alive
248 was not easy and was based on color and size. Therefore, some fetal mice classified as dead

might have been alive.

In conclusion, in the current study we have focused on the examination of the effects of *Atg9a* deficiency in fetal mice on fetal growth and survival. We demonstrated that *Atg9a*-knockout (*Atg9a* $^{-/-}$) fetal mice were likely to show growth restriction, especially in the presence of maternal hypertension. This suggests that dysfunction of fetal autophagic machinery causes lower fetal body weight. In addition, the results of the study indicated that fetal mice devoid of *Atg9a* had an increased likelihood of dying *in utero*, similar to the observations reported previously for autophagy-defective *beclin 1*$^{-/-}$ mice [14].

Conflict of Interest

None declared.

References

[1] Mizushima N, Ohsumi Y, Yoshimori T: Autophagosome formation in mammalian cells. Cell Struct Funct 2002, 27:421-429.

[2] Lum JJ, DeBerardinis RJ, Thompson CB: Autophagy in metazoans: cell survival in the land of plenty. Nat Rev Mol Cell Biol 2005, 6:439-448.

[3] Xie Z, Klionsky DJ: Autophagosome formation: core machinery and adaptations. Nat Cell Biol 2007, 9:1102-1109.

[4] Klionsky DJ, Cregg JM, Dunn WA, Emr SD, Sakai Y, Sandoval IV, Sibirny A, Subramani S, Thumm M, Veenhuis M, Ohsumi Y: A unified nomenclature for yeast autophagy-related genes. Dev Cell 2003, 5:539-545.

[5] Tsukada M, Ohsumi Y: Isolation and characterization of autophagy-defective mutants of Saccharomyces cerevisiae. FEBS Lett 1993, 333:169-174.

[6] Kuma A, Hatano M, Matsui M, Yamamoto A, Nakaya H, Yoshimori T, Ohsumi Y, Tokuhisa T, Mizushima N: The role of autophagy during the early neonatal starvation period. Nature 2004, 432:1032-1036.

[7] Komatsu M, Waguri S, Ueno T, Iwata J, Murata S, Tanida I, Ezaki J, Mizushima N, Ohsumi Y, Uchiyama Y, et al: Impairment of starvation-induced and constitutive autophagy in Atg7-deficient mice. J Cell Biol 2005, 169:425-434.

[8] Saitoh T, Fujita N, Jang MH, Uematsu S, Yang BG, Satoh T, Omori H, Noda T, Yamamoto N, Komatsu M, et al: Loss of the autophagy protein Atg16L1 enhances endotoxin-induced IL-1beta production. Nature 2008, 456:264-268.

283 [9] Saitoh T, Fujita N, Hayashi T, Takahara K, Satoh T, Lee H, Matsunaga K, Kageyama S,
284 Omori H, Noda T, et al: Atg9a controls dsDNA-driven dynamic translocation of STING
285 and the innate immune response. Proc Natl Acad Sci U S A 2009, 106:20842-20846.
286 [10] Sou YS, Waguri S, Iwata J, Ueno T, Fujimura T, Hara T, Sawada N, Yamada A,
287 Mizushima N, Uchiyama Y, et al: The Atg8 conjugation system is indispensable for
288 proper development of autophagic isolation membranes in mice. Mol Biol Cell 2008,
289 19:4762-4775.
290 [11] Albaiges G, Missfelder-Lobos H, Lees C, Parra M, Nicolaides KH: One-stage screening
291 for pregnancy complications by color Doppler assessment of the uterine arteries at 23
292 weeks' gestation. Obstet Gynecol 2000, 96:559-564.
293 [12] Steegers EA, von Dadelszen P, Duvekot JJ, Pijnenborg R: Pre-eclampsia. Lancet 2010,
294 376:631-644.
295 [13] Contro E, Cha DH, De Maggio I, Ismail SY, Falcone V, Gabrielli S, Farina A: Uterine
296 artery Doppler longitudinal changes in pregnancies complicated with intrauterine growth
297 restriction without preeclampsia. Prenat Diagn 2014.
298 [14] Yue Z, Jin S, Yang C, Levine AJ, Heintz N: Beclin 1, an autophagy gene essential for
299 early embryonic development, is a haploinsufficient tumor suppressor. Proc Natl Acad
300 Sci U S A 2003, 100:15077-15082.
301 [15] Hatada I, Mukai T: Genomic imprinting of p57KIP2, a cyclin-dependent kinase inhibitor, in
302 mouse. Nat Genet 1995, 11:204-206.
303 [16] Matsuoka S, Thompson JS, Edwards MC, Bartletta JM, Grundy P, Kalikin LM, Harper

JW, Elledge SJ, Feinberg AP: Imprinting of the gene encoding a human cyclin-dependent kinase inhibitor, p57KIP2, on chromosome 11p15. Proc Natl Acad Sci U S A 1996, 93:3026-3030.

[17] Kanayama N, Takahashi K, Matsuura T, Sugimura M, Kobayashi T, Moniwa N, Tomita M, Nakayama K: Deficiency in p57Kip2 expression induces preeclampsia-like symptoms in mice. Mol Hum Reprod 2002, 8:1129-1135.

[18] Takahashi K, Nakayama K: Mice lacking a CDK inhibitor, p57Kip2, exhibit skeletal abnormalities and growth retardation. J Biochem 2000, 127:73-83.

[19] Yamada T, Carson AR, Caniggia I, Umebayashi K, Yoshimori T, Nakabayashi K, Scherer SW: Endothelial nitric-oxide synthase antisense (NOS3AS) gene encodes an autophagy-related protein (APG9-like2) highly expressed in trophoblast. J Biol Chem 2005, 280:18283-18290.

[20] Oh SY, Choi SJ, Kim KH, Cho EY, Kim JH, Roh CR: Autophagy-related proteins, LC3 and Beclin-1, in placentas from pregnancies complicated by preeclampsia. Reprod Sci 2008, 15:912-920.

[21] Hung TH, Chen SF, Lo LM, Li MJ, Yeh YL, Hsieh TT: Increased autophagy in placentas of intrauterine growth-restricted pregnancies. PLoS One 2012, 7:e40957.

[22] Chang YL, Wang TH, Chang SD, Chao AS, Hsieh PC, Wang CN: Increased autophagy in the placental territory of selective intrauterine growth-restricted monochorionic twins. Prenat Diagn 2013, 33:187-190.

[23] Curtis S, Jones CJ, Garrod A, Hulme CH, Heazell AE: Identification of autophagic

vacuoles and regulators of autophagy in villous trophoblast from normal term pregnancies and in fetal growth restriction. J Matern Fetal Neonatal Med 2013, 26:339-346.

[24] Akaishi R, Yamada T, Nakabayashi K, Nishihara H, Furuta I, Kojima T, Morikawa M, Fujita N, Minakami H: Autophagy in the placenta of women with hypertensive disorders in pregnancy. Placenta 2014, 35:974-980.

Figure captions

Fig. 1. Exemplary images of fetuses at 17.5 day post coitum. A/ *Atg9a* $^{-/-}$ fetuses judged as dead, B/ *Atg9a* $^{-/-}$ fetuses with growth retardation, C/ *Atg9a* $^{+/+}$ fetuses with normal growth. The *Atg9a* genotypes of the fetuses were determined by PCR of mouse tail DNA according to the presence or absence of wild type (WT) and knockout (KO) alleles.

Fig. 2. Systolic blood pressure (mean ± SD) in *Atg9a*$^{+/-}$/*p57*$^{Kip+/-}$ and *Atg9a*$^{+/-}$ pregnant mice. The numbers of pregnant mice are indicated in parentheses. *$P < 0.05$ between the two examined groups of mice; †$P < 0.05$ between a particular day post coitum (dpc) and a pre-pregnancy day (SBP baseline).

Fig. 3. Expression of *Atg9a* mRNA in the placentas of *Atg9a*$^{+/+}$, *Atg9a* $^{+/-}$ *and Atg9a* $^{-/-}$ mice. The mice were sacrificed at 15.5 day post coitum; the numbers of pregnant mice are indicated in parentheses. Different superscripts mean significant differences (P<0.05).

Fig. 4. Expression of *Atg9b* mRNA, Atg9b protein and LC3-II protein in placentas with *Atg9a*$^{+/+}$ and *Atg9a*$^{-/-}$ genotypes. The pregnant mice were sacrificed at 17.5 day post coitum. Please refer to Table 1 for group (A1, A2, B1, and B2) definition. Different superscripts mean significant differences (P<0.05).

Fig. 5. Fetal body weight in the A1+A2 (normotensive) and B1+B2 (hypertensive) mice on 13.5, 15.5, and 17.5 days post coitum (dpc). Numbers of fetuses are presented in parentheses. Upper and lower ends of the box and horizontal line inside the box indicate 75th percentile, 25th percentile, and median values, respectively. *$P < 0.05$ between the two compared groups. Please refer to Table 1 for group (A1, A2, B1, and B2) definition.

Fig. 6. Fetal body weight in the A1+B1 and A2+B2 mice on 13.5, 15.5, and 17.5 days post coitum (dpc). Numbers of fetuses are presented in parentheses. Upper and lower ends of the box and horizontal line inside the box indicate 75th percentile, 25th percentile, and median values, respectively. *$P < 0.05$ between the two compared groups. Please refer to Table 1 for group (A1, A2, B1, and B2) definition.

Fig. 7. Fetal body weight in the A1, A2, B1 and B2 mice on 13.5, 15.5, and 17.5 days post coitum (dpc). Numbers of fetuses are presented in parentheses. Upper and lower ends of the box and horizontal line inside the box indicate 75th percentile, 25th percentile, and median values, respectively. *$P < 0.05$ between the two compared groups. Please refer to Table 1 for group (A1, A2, B1, and B2) definition.

372 Fig. 1.

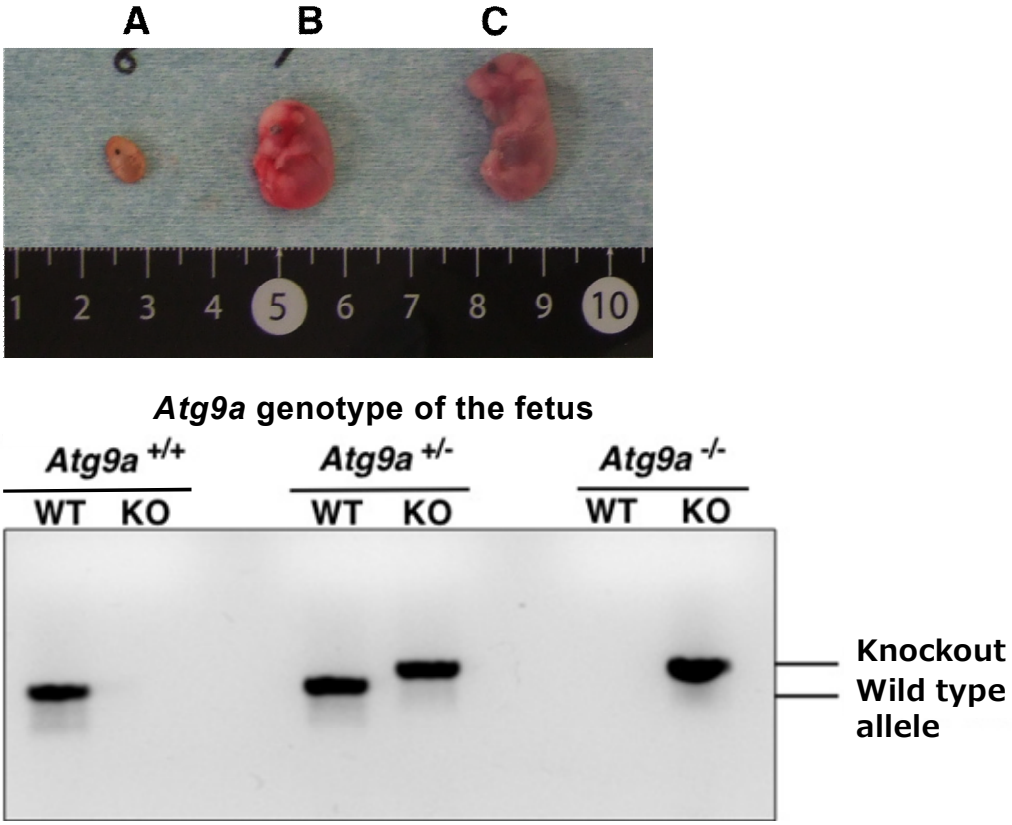

373

374

375 Fig. 2.

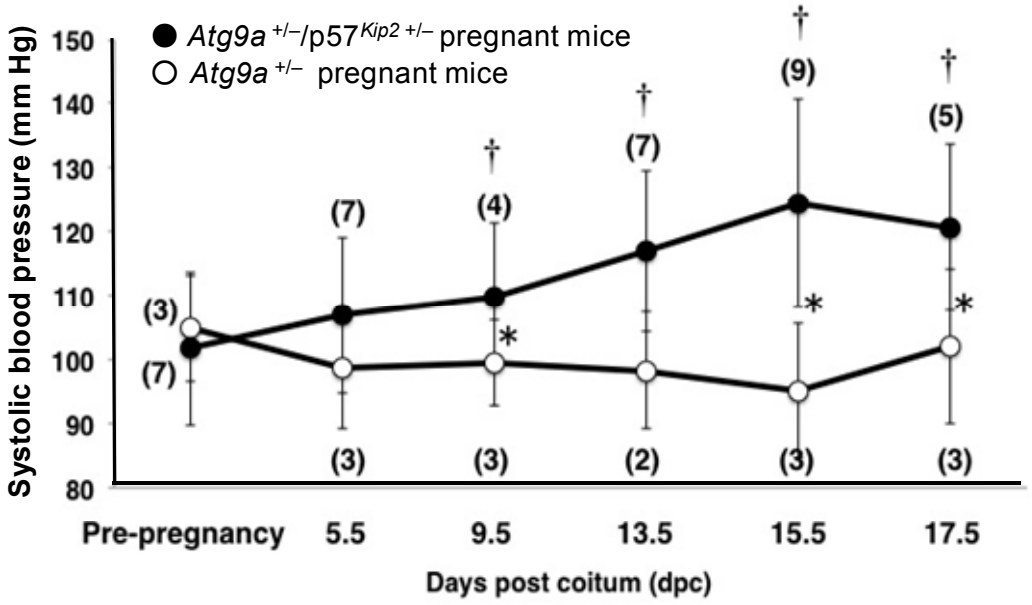

376

377

378

379 Fig. 3.

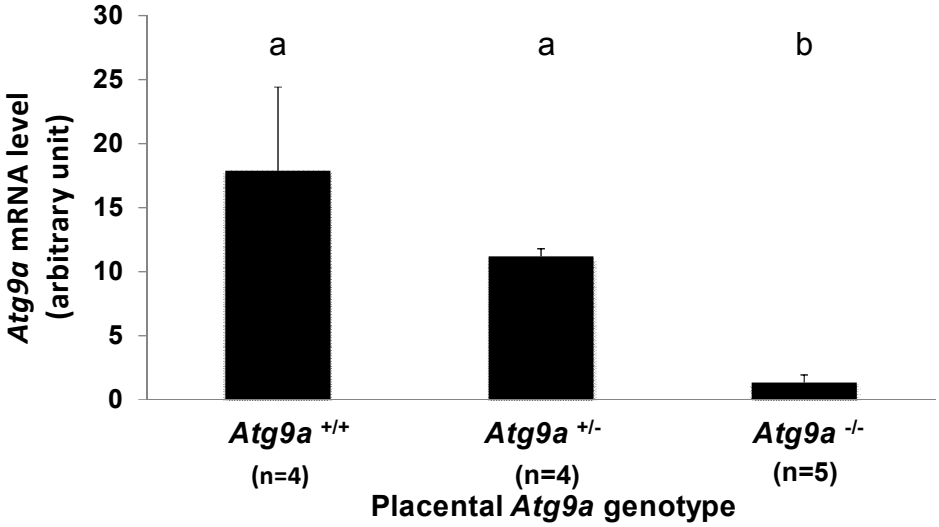

380

381

382

383 Fig. 4.

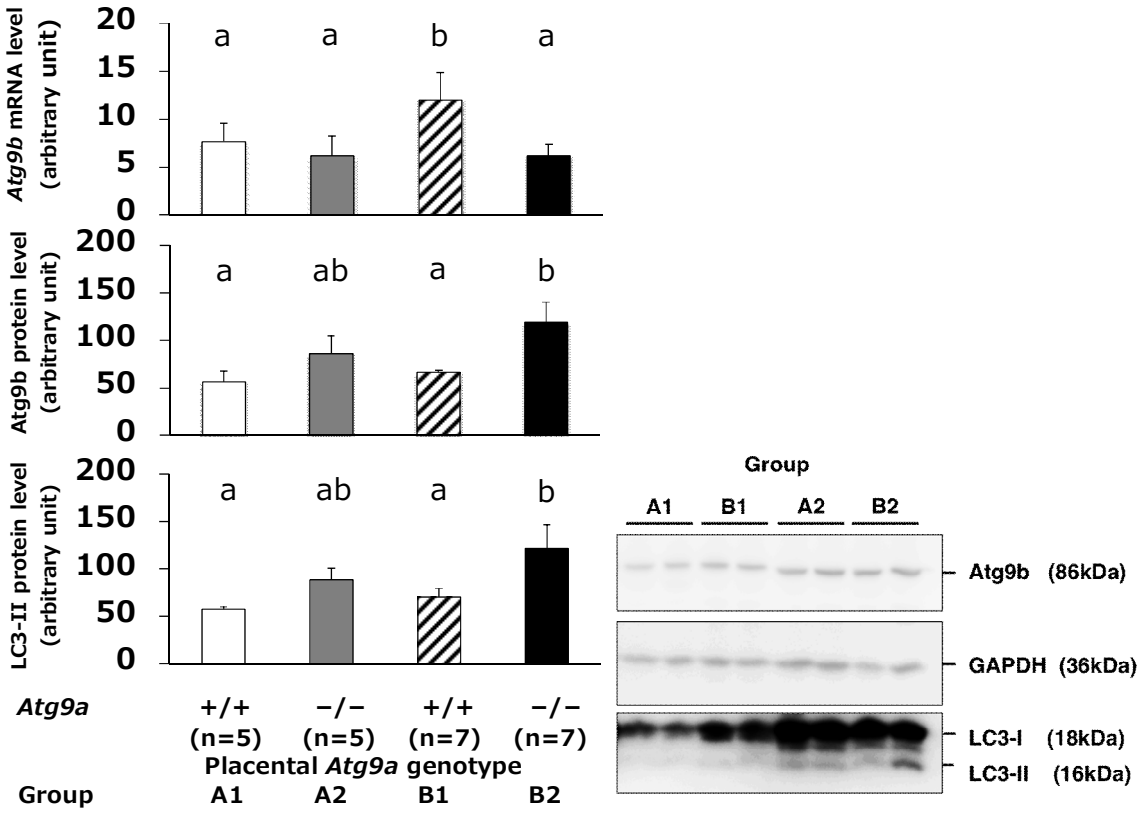

384

385

386

387 Fig. 5.

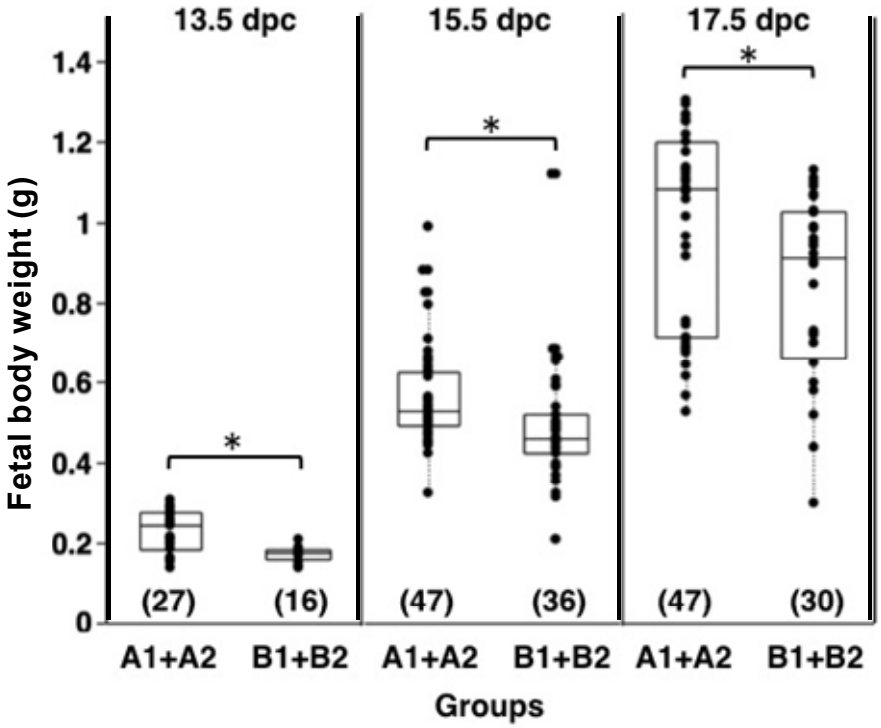

388

389

390

391 Fig. 6.

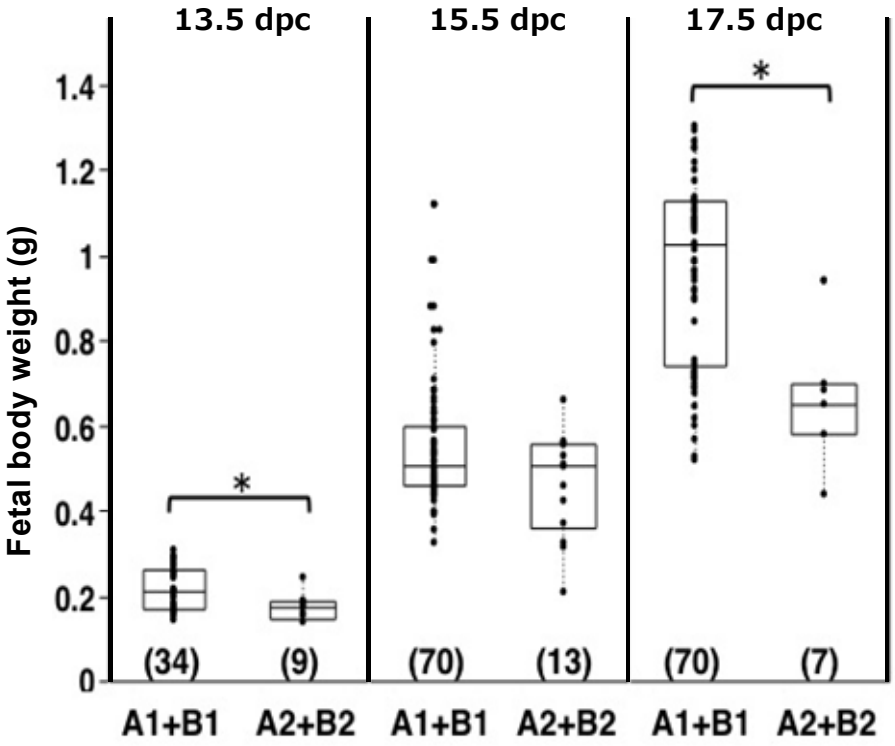

392

393

394 Fig. 7.

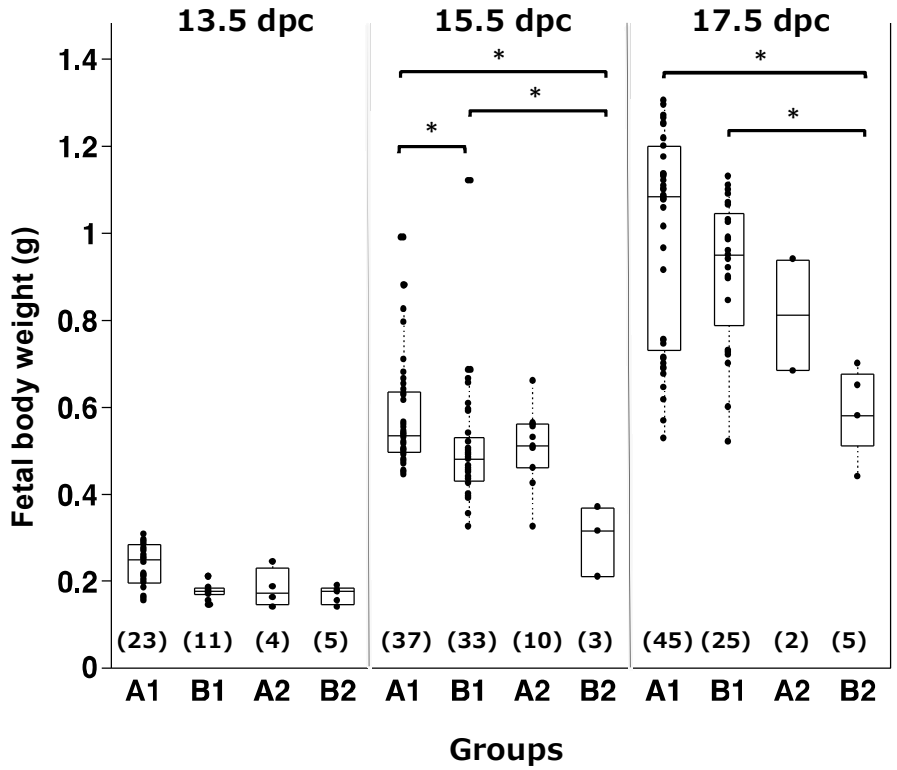
13.5 dpc
15.5 dpc
17.5 dpc
Fetal body weight (g)
1.4
1.2
1
0.8
0.6
0.4
0.2
0
*
*
*
*
*
(23) (11) (4) (5) (37) (33) (10) (3) (45) (25) (2) (5)
A1 B1 A2 B2 A1 B1 A2 B2 A1 B1 A2 B2
Groups

395

Table 1. Mating patterns and fetal *Atg9a* genotype

Mating (male × female)		Fetal genotype
Group A1	$Atg9a^{+/-} \times Atg9a^{+/-}$	$Atg9a^{+/+}$, $Atg9a^{+/-}$
Group A2	$Atg9a^{+/-} \times Atg9a^{+/-}$	$Atg9a^{-/-}$
Group B1	$Atg9a^{+/-} \times Atg9a^{+/-}/p57^{Kip2\,+/-}$*	$Atg9a^{+/+}$, $Atg9a^{+/-}$
Group B2	$Atg9a^{+/-} \times Atg9a^{+/-}/p57^{Kip2\,+/-}$*	$Atg9a^{-/-}$

*$p57^{Kip2\,+/-}$: heterozygous, devoid of the imprinted paternal allele

Table 2**.** Effects of fetal *Atg9a* genotype on the number of live or dead fetal mice and **the** intrauterine fetal death (IUFD) rate

Dams: *Atg9a* $^{+/-}$ (normotensive group)				
Fetal genotype	n	*Atg9a* $^{+/+}$ (A1)	*Atg9a* $^{+/-}$ (A1)	*Atg9a* $^{-/-}$ (A2)
13.5 dpc	4	12/0	11/3	4/0
15.5 dpc	4	21/0	16/3	10/1
17.5 dpc	5	14/1	31/2	2/6
IUFD rate		2.1% (1/48)	12% (8/66)	30% (7/23)
Dams: *Atg9a* $^{+/-}$/p57$^{Kip2\,+/-}$ (hypertensive group)				
Fetal genotype	n	*Atg9a* $^{+/+}$ (B1)	*Atg9a* $^{+/-}$ (B1)	*Atg9a* $^{-/-}$ (B2)
13.5 dpc	2	3/0	8/0	5/0
15.5 dpc	6	9/0	24/4	3/1
17.5 dpc	5	9/0	16/5	5/2
IUFD rate		0.0% (0/21)	16% (9/57)	19% (3/16)
Overall number of fetuses		69 (68/1)	123 (106/17)	39 (29/10)
Overall IUFD rate		1.4% (1/69)[a]	14% (17/123) [b]	26% (10/39) [c]

dpc - day *post coitum*; **n -** number of dams sacrificed.

$P < 0.05$ for a vs. b, a vs. c; and a + b (18/192) vs. c; Fisher's exact test with Bonferroni correction.